Sigmoidal kinetic model for two co-operative substrate-binding sites in a cytochrome P450 3A4 active site: an example of the metabolism of diazepam and its derivatives

Magang SHOU*[1], Qin MEI*, Michael W. ETTORE, JR.*, Renke DAI†, Thomas A. BAILLIE* and Thomas H. RUSHMORE*

*Department of Drug Metabolism, Merck Research Laboratories, West Point, PA 19486, U.S.A., and †Laboratory of Molecular Carcinogenesis, National Cancer Institute, NIH, Bethesda, MD 20892, U.S.A.

Cytochrome P450 3A4 (CYP3A4) plays a prominent role in the metabolism of a vast array of drugs and xenobiotics and exhibits broad substrate specificities. Most cytochrome P450-mediated reactions follow simple Michaelis–Menten kinetics. These parameters are widely accepted to predict pharmacokinetic and pharmacodynamic consequences *in vivo* caused by exposure to one or multiple drugs. However, CYP3A4 in many cases exhibits allosteric (sigmoidal) characteristics that make the Michaelis constants difficult to estimate. In the present study, diazepam, temazepam and nordiazepam were employed as substrates of CYP3A4 to propose a kinetic model. The model hypothesized that CYP3A4 contains two substrate-binding sites in a single active site that are both distinct and co-operative, and the resulting velocity equation had a good fit with the sigmoidal kinetic observations. Therefore, four pairs of the kinetic estimates (K_{S1}, k_α, K_{S2}, k_β, K_{S3}, k_δ, K_{S4} and k_γ) were resolved to interpret the features of binding affinity and catalytic ability of CYP3A4. Dissociation constants K_{S1} and K_{S2} for two single-substrate-bound enzyme molecules (SE and ES) were 3–50-fold greater than K_{S3} and K_{S4} for a two-substrate-bound enzyme (SES), while respective rate constants k_δ and k_γ were 3–218-fold greater than k_α and k_β, implying that access and binding of the first molecule to either site in an active pocket of CYP3A4 can enhance the binding affinity and reaction rate of the vacant site for the second substrate. Thus our results provide some new insights into the co-operative binding of two substrates in the inner portions of an allosteric CYP3A4 active site.

Key words: cDNA expression, drug interaction, drug metabolism, enzyme kinetics, monoclonal antibody.

INTRODUCTION

The cytochrome P450s (P450s) are a superfamily of enzymes that catalyse the metabolism of a variety of endogenous and exogenous compounds [1–4]. P450 isoforms possess identical prosthetic groups but different apoprotein structures that are responsible for the broad and overlapping substrate specificities. Most P450-mediated reactions follow simple Michaelis–Menten kinetics from which kinetic constants (K_m and V_{max}) are easily derived. If the addition of an effector (inhibitor or activator) to a P450 reaction results in a competitive inhibition or activation of the enzyme reaction, a value for K_i or K_A (usually $\alpha < 1$ and $\beta > 1$) can be determined. These kinetic parameters are accepted widely to predict *in vivo* pharmacokinetic and pharmacodynamic consequences caused by exposure to one or multiple drugs.

However, some P450s display non-Michaelis–Menten kinetics, apparently resulting from an allosteric effect that commonly yields a sigmoidal velocity saturation curve. Most of the examples reported to date have been attributed to cytochrome P450 3A4 (CYP3A4), e.g. the metabolism of aflatoxin B1 [5], steroids [6,7], carbamazepine [8,9] and amitriptyline [10]. The existence of allosteric kinetics in Nature may be rationalized in terms of the mechanism of metabolic control, e.g. feedback inhibition of the first reaction of a sequence by the ultimate product (negative feedback). At intermediate specific velocities of the kinetics, the sigmoidal response provides a much more sensitive control of the reaction rate than the normal hyperbolic velocity by variations in the substrate concentration. However, in a low substrate concentration range, velocity response is much slower than that observed for normal kinetics. Due to co-operative binding of enzyme(s) with two or more binding sites, the observed kinetics cannot be interpreted easily by a simple Michaelis–Menten equation.

A P450 isoform that possesses two binding sites in a catalytic pocket can generate two different kinetic profiles (non-co-operative and co-operative). The former suggests that both sites are identical and independent (Scheme 1, $\alpha = 1$). However, all dissociation (K_S) and rate constants (k_p) expressed at different equilibration steps are equivalent. A velocity equation can be derived as eqn. (1) that reduces further to eqn. (2):

$$\frac{v}{V_{max}} = \frac{\frac{[S]}{K_S} + \frac{[S]^2}{K_S^2}}{1 + \frac{2[S]}{K_S} + \frac{[S]^2}{K_S^2}} \quad (1)$$

$$\frac{v}{V_{max}} = \frac{[S]}{K_S + [S]} \quad (2)$$

Thus the kinetics of two identical and independent binding sites on an enzyme basically follow the Michaelis–Menten equation (eqn. 2) and display an essentially hyperbolic curve. More concisely, the binding of one substrate has no effect on the dissociation and rate constants of the other site.

In contrast, if the binding of one substrate molecule induces structural or electronic changes of the enzyme that result in an

Abbreviations used: P450, cytochrome P450; CYP3A4, cytochrome P450 3A4; CYP-OR, human cytochrome P450 oxidoreductase; mAb, monoclonal antibody; DZ, diazepam; TMZ, temazepam; NDZ, nordiazepam; OX, oxazepam; KPi, potassium phosphate buffer.

[1] To whom correspondence should be addressed (e-mail magang_shou@merck.com).

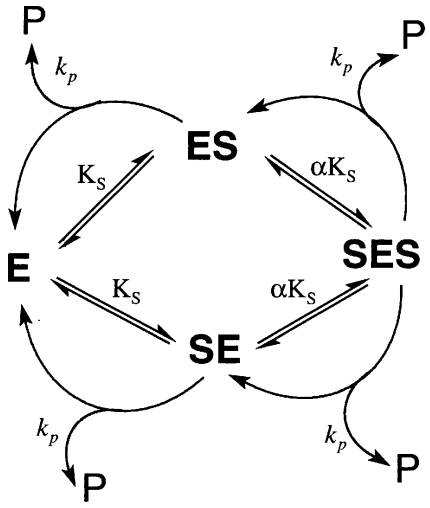

Scheme 1 A kinetic model for an enzyme with two binding sites

Both sites are identical and independent and are expressed as two ways of arranging S, as ES and SE. The rate (k_p) and dissociation (K_S) constants for all product-forming species in the model are identical. When $\alpha = 1$, the two binding sites are identical and non-cooperative and the velocity equations are expressed in eqns. (1) and (2). When $\alpha \neq 1$, the two binding sites are identical and co-operative, e.g. the binding of one substrate changes the affinity of the vacant site (K_S) for a second substrate by a factor, α, and the k_p values for all species are same. This is shown in eqn. (3).

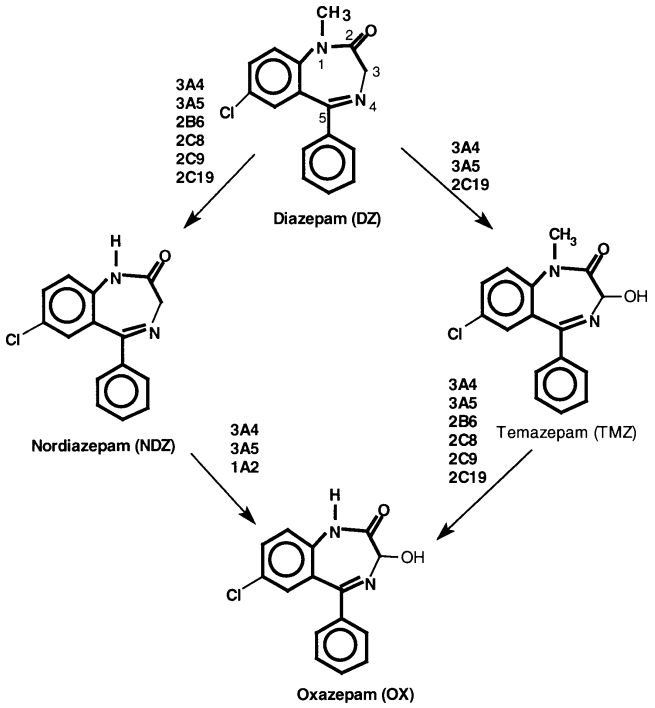

Scheme 2 Metabolic pathways of DZ by P450s

altered affinity and/or increase in the rate of product formation for a second substrate-binding site, the velocity curve will no longer follow Michaelis–Menten kinetics, but will display the kinetic characteristics of an allosteric enzyme (substrate activation, so-called co-operative binding). The Hill equation is usually employed to generate kinetic parameters and gives an appropriate fit to experimental data [11]. The model postulates that an enzyme is considered to have two identical substrate-binding sites with one identical rate constant for the breakdown of all enzyme–substrate species (Scheme 1, $\alpha \neq 1$). If the enzyme-mediated reaction is significantly co-operative, the binding of one substrate molecule changes the affinity by a factor, α, and the velocity equation becomes:

$$v = \frac{V_{max}\left(\frac{[S]}{K_S} + \frac{[S]^2}{\alpha K_S^2}\right)}{1 + \frac{2[S]}{K_S} + \frac{[S]^2}{\alpha K_S^2}} \quad (3)$$

If the Hill equation is used to consider n equivalent substrate-binding sites on an enzyme and the co-operativity in substrate binding is significant, the concentrations of enzyme–substrate complexes containing less than n molecules of substrate will be negligible at any [S]. Thus the Hill equation for an n-binding-site enzyme reduces to:

$$v = \frac{V_{max}[S]^n}{K' + [S]^n} \quad (4)$$

K' is a constant comprising the interaction factors and no longer equals K_m, which is the substrate concentration that yields half-maximal velocity except when $n = 1$. Thus the K' value that was used as K_m, C_{50} or S_{50} of co-operative kinetics of P450-mediated reactions in previous reports is inappropriate [5,12,13].

The kinetic models for simultaneous substrate binding or substrate–effector binding to a P450 active site were proposed to explain the non-Michaelis–Menten kinetics [9,14]. The two-site model described sigmoidal kinetic characteristics for carbamazepaine metabolism by CYP3A4, naphthalene metabolism by P450 2B6, -2C8, -2C9 and -3A5 and dapsone metabolism by CYP2C9, as well as the kinetics of the phenanthrene–α-naphthoflavone interaction. Accordingly, the velocity equation for the two-site binding model was developed to fit experimental data (eqn. 5) and kinetic estimates for two binding sites (e.g. K_{m1}, K_{m2}, V_{max1} and V_{max2}) were determined.

$$v = \frac{\frac{V_{max1}[S]}{K_{m1}} + \frac{V_{max2}[S]^2}{K_{m1}K_{m2}}}{1 + \frac{[S]}{K_{m1}} + \frac{[S]^2}{K_{m1}K_{m2}}} \quad (5)$$

Although these equations were applied to account for many sigmoidal kinetic observations for P450-mediated reactions, the kinetic parameters determined may remain controversial and may be inadequate to fully interpret the discrimination between all enzyme–substrate species in the allosteric kinetics. Based on our current understanding of known P450 crystal structures, the properties of physical chemistry for two binding sites in a P450 active site, e.g. steric hindrance, hydrophobic interaction and electronic characteristics, could not be identical. Therefore, the K_{m1} may not be appropriate to represent both $E + S \leftrightharpoons SE$ and $E + S \leftrightharpoons ES$ equilibria, and the K_{m2} may not be for both $ES + S \leftrightharpoons SES$ and $SE + S \leftrightharpoons SES$ [9]. Accordingly, rate constants for the breakdown of all three product-forming species (SE, ES and SES) to product(s) can vary. In an attempt to better characterize the allosteric CYP3A4 enzyme that gives a sigmoidal kinetic response, a two-site model was proposed and its kinetic predictions were determined quantitatively.

In the present study, diazepam (DZ) and two of its known metabolites, nordiazepam (NDZ) and temazepam (TMZ), were employed as substrates for establishing an allosteric kinetic

model. The metabolism of DZ by human and rat liver microsomes has been found to exhibit sigmoidal kinetics in several reports [12,15–17]. The primary routes of P450-mediated biotransformation of DZ are shown in Scheme 2 [12,15–21]. Our study confirmed that CYP3A4 is an allosteric enzyme responsible for sigmoidal kinetics in the metabolism of DZ by human liver microsomes and cDNA-expressed CYP3A4, and described an allosteric kinetic model for the simultaneous binding of two substrate molecules in a single CYP3A4 active site. A velocity equation was derived to fit the experimental data and kinetic constants were estimated quantitatively to interpret the co-operative binding of DZ and its derivatives to the allosteric CYP3A4 enzyme.

MATERIALS AND METHODS

Materials

DZ, TMZ, NDZ and NADPH were purchased from Sigma (St. Louis, MO, U.S.A.). An inhibitory anti-CYP3A4 monoclonal antibody (mAb) was purchased from Gentest Corp. (Woburn, MA, U.S.A.) and characterized as reported previously [22]. Benz[*a*]anthracene *trans*-5,6-dihydrodiol was obtained from the National Cancer Institute Chemical Carcinogen Repository (Kansas City, MO, U.S.A.).

CYP3A4 expression in baculovirus system

Plasmids pGem-7/CYP3A4 and pGem-3Z/CYP-OR containing the full-length cDNAs for CYP3A4 [23] and human P450 oxidoreductase (CYP-OR) [24] were provided by Dr. Frank J. Gonzalez (National Cancer Institute, Bethesda, MD, U.S.A.). The entire coding region of each cDNA was excised from the vectors and inserted into baculovirus shuttle vector, pBlueBac (CYP3A4, *Xba*I/*Kpn*I; and CYP-OR, *Eco*RI). Recombinant virus was constructed according to the manufacturer's procedure (Invitrogen, Carlsbad, CA, U.S.A.) and isolated using blue-gal for colour selection of recombinant virus. After two runs of plaque purification, the virus was then amplified in high-titre stock for CYP3A4 protein expression. Sf21 insect cells (Invitrogen) were grown at 27 °C in complete Sf900 medium (Gibco BRL, Gaithersburg, MD, U.S.A.) to a density of 2×10^6 cells/ml (400 ml in total) in 1-litre spinner flasks (Bellco Glass, Vineland, NJ, U.S.A.) with enlarged blades at 90 rev./min. Cells were infected at approx. 1.0 multiplicity of infection of virus encoding CYP3A4 and at 0.1 multiplicity of infection of virus encoding CYP-OR. Then, 1 μg of hemin/ml of medium in the form of a hemin–albumin complex was added. After 72 h, cells were harvested by centrifugation and resuspended with 20 % glycerol in 0.1 M KPi (potassium phosphate buffer). The total P450 content was measured by the CO-difference spectrum [25]. Microsomes were prepared as described below and the resulting protein concentration was determined with bicinchoninic acid according to the manufacturer's directions (Pierce, Rockford, IL, U.S.A.). The molar ratio of CYP3A4 to CYP-OR in microsomal preparation was 1:2.8 and the specific activity of CYP3A4 in testosterone 6β-hydroxylation was 42 nmol of product formed/min per nmol of P450.

Microsomal preparation from human livers and Sf21 cells expressing CYP3A4

Normal liver specimens from six subjects aged from 20 to 55 (two female and four male Caucasians) were provided by the National Cancer Institute Cooperative Human Tissue Network (Philadelphia, PA, U.S.A.). Clinical information on the donors was provided indicating the causes of death to be automobile accidents (three cases), coronary artery disease (one case) and respiratory failure (two cases). The donors were non-smokers and non-alcoholics and their renal- and hepatic-function tests were normal. Microsomes were prepared as described previously [26] and were reconstituted in a buffer (pH 7.4) containing 0.25 M sucrose, 1 mM EDTA, 0.5 mM dithiothreitol, 1.15 % KCl and 0.1 M KPi. Six individual human liver microsomal preparations were pooled at an equivalent amount of P450 and stored at −80 °C until used.

Metabolism of benzodiazepines

Incubation mixtures (1 ml) contained microsomal protein (50–100 pmol of P450 from Sf21 cells or human liver microsomes), 0.1 M KPi buffer (pH 7.5) and substrate (DZ, TMZ or NDZ) at various concentrations. The mixture was preincubated for 2 min at 37 °C in a shaking water bath, and the reaction was initiated by addition of 1 mM NADPH and incubated for 15 or 20 min. The reactions were arrested by 8 vol. of methylene chloride and an internal standard was added for metabolite quantification. For enzyme kinetics, approximately 40 different substrate concentrations were chosen over the range of 2–1200 μM. For mAb-inhibition studies, anti-CYP3A4 mAb (30 nM) was preincubated with enzyme at room temperature for 5 min before the addition of substrate and NADPH. For time-course studies, samples were collected at 2.5, 5, 10, 20, 30 and 60 min at two concentrations of DZ (20 and 500 μM) for assay of metabolite production. The remaining substrate and metabolites formed were extracted with 8 vol. of methylene chloride and centrifuged for 10 min (500 ***g***). The organic phase was allowed to evaporate to dryness under a stream of nitrogen and the residue was dissolved in 80 % methanol in water for HPLC analysis.

HPLC

HPLC was performed on a Hewlett-Packard model 1100 liquid chromatograph. DZ and its metabolites were separated on a Vydac C_{18} column [210TP54, 5-μm particles, 4.6 mm (inner diameter) × 25 cm; The Separations Group, Hesperia, CA, U.S.A.]. The mobile phase was acetonitrile/methanol/H_2O (20:30:50, v/v/v) at a flow rate of 1 ml/min. The eluate was monitored by UV light at 232 nm. Calibration curves and quantification of TMZ, NDZ and oxazepam (OX) relative to a known amount of the appropriate internal standard (DZ for TMZ and NDZ metabolism and benz[*a*]anthracene *trans*-5,6-dihydrodiol for DZ metabolism) were established from the areas under the chromatographic peaks at 232 nm.

Hypothesis of co-operative kinetic model

Human P450s are believed to be monomers that have one active site per enzyme molecule, as suggested by the crystal structures of P450cam and P450BM3. We proposed the two-binding site model, which states that two substrates can bind simultaneously to different portions of the active site. Two binding sites in the model are co-operative, meaning that occupancy of either site by one substrate changes the binding affinity of the vacant second site. This means that the resulting kinetic properties of two occupied substrate-binding sites no longer resemble those of the one-substrate-bound enzyme. The hypothesis is based on the assumption that a rapid equilibrium is formed between the enzyme and substrate, which react rapidly to form enzyme–substrate complexes. The kinetic scheme for an enzyme with two

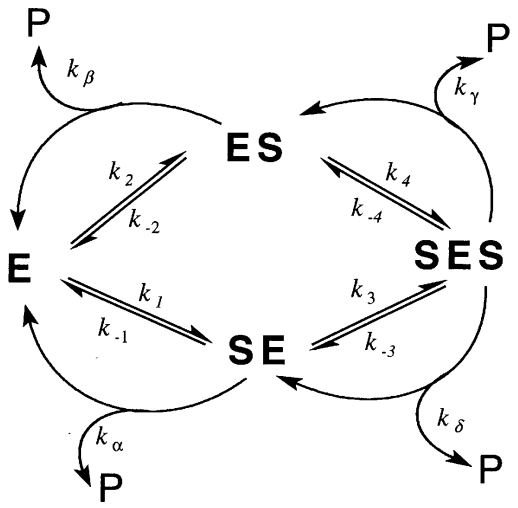

Scheme 3 Proposed allosteric kinetic scheme for an enzyme with two binding sites in a CYP3A4 active site

Velocity equation was derived as shown in eqn. (6).

binding sites is given in Scheme 3. All species in the reaction are at equilibrium, i.e. the rate at which each enzyme–substrate complex dissociates is much faster than the rate at which it breaks down to product(s). Thus the K_s values can be expressed by $K_{s1} = k_{-1}/k_1$, $K_{s2} = k_{-2}/k_2$, $K_{s3} = k_{-3}/k_3$ and $K_{s4} = k_{-4}/k_4$, respectively. At steady state, the rates of formation and decomposition of enzyme–substrate complexes are equivalent, e.g. $(+\mathrm{d[ES]/d}t) = k_1[\mathrm{E}][\mathrm{S}] = (-\mathrm{d[ES]/d}t) = (k_{-1} + k_\alpha)[\mathrm{ES}]$. Thus product formation should be linear as a function of reaction time. The model differentiates all possible equilibration and rate steps of enzyme–substrate complexes on two binding sites to describe co-operative effects of the reaction, e.g. K_{s1}, K_{s2}, K_{s3}, K_{s4}, k_α, k_β, k_δ and k_γ. Hence, dissociations of enzyme–substrate forms and rates of product-forming species in the model can be distinct from each other. Therefore, the velocity equation is written from the model as shown below (eqn. 6). The hypothesis was tested to determine whether the derived equation fits with the sigmoidal kinetics exhibited in the metabolism of DZ and its derivatives by human CYP3A4 and liver microsomes.

$$\frac{v}{[\mathrm{E}]_{\mathrm{total}}} = \frac{\dfrac{k_\alpha}{K_{s1}} + \dfrac{k_\beta}{K_{s2}} + \dfrac{[\mathrm{S}]}{K_{s1}K_{s3}}(k_\delta + k_\gamma)}{\dfrac{1}{[\mathrm{S}]} + \dfrac{1}{K_{s1}} + \dfrac{1}{K_{s2}} + \dfrac{[\mathrm{S}]}{K_{s2}K_{s4}}} \quad (6)$$

Kinetic derivation and analysis

A velocity equation was derived on the assumption of rapid equilibration of all enzyme species (Scheme 3) and was fitted to sigmoidal curves observed in our experiments. The values of all kinetic parameters were adjusted with an iteration that best fitted the data by using a program of the Marquardt–Levenberg non-linear least-squares algorithm [27]. Plots of equations were

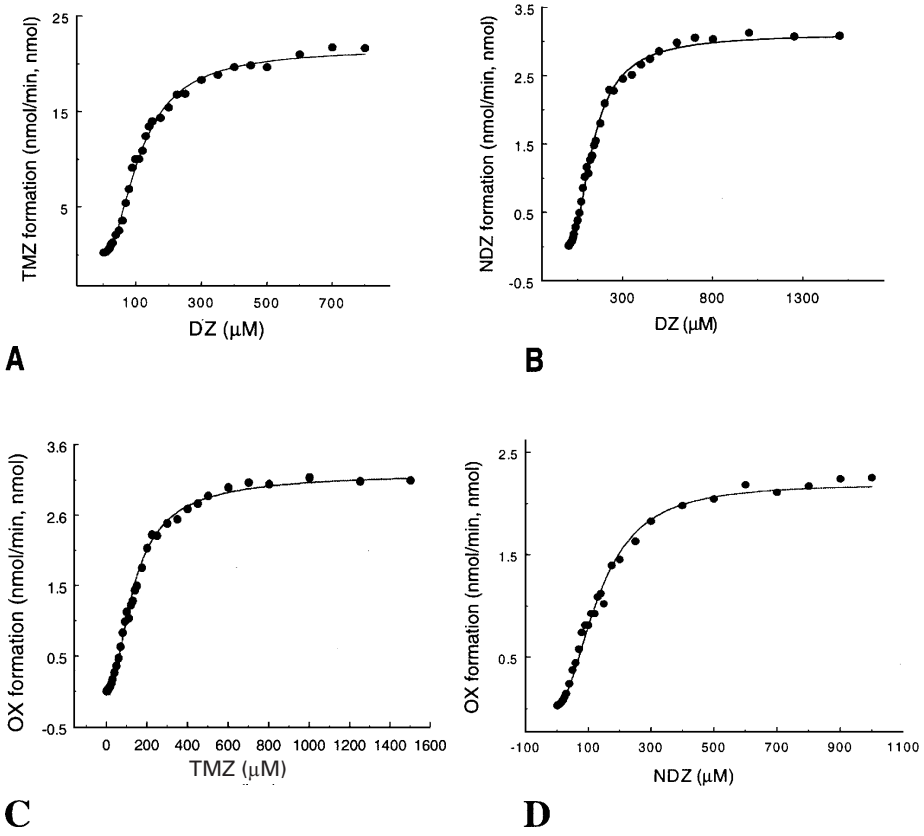

Figure 1 Sigmoidal saturation curve of *v* versus [S] for the recombinant CYP3A4-catalysed metabolism of DZ, TMZ and NDZ

(**A**) DZ conversion into TMZ; (**B**) DZ conversion into NDZ; (**C**) TMZ conversion into OX; and (**D**) NDZ conversion into OX.

prepared and fits of kinetic-parameter statistics were determined by a regression analysis using Axum 5.0 software (Mathsoft, Cambridge, MA, U.S.A.).

RESULTS

Time-dependent formation of DZ products

Studies on the time-dependent formation of TMZ during the metabolism of DZ by CYP3A4 were performed at concentrations of 20 and 500 μM and indicated linearity up to at least 20 min of incubation at 37 °C (results not shown). Less than 10 % of substrate was consumed and secondary metabolism did not occur during the course of the incubation. The linearity of product formation as a function of incubation time suggests that CYP3A4-catalysed reactions, where the initial substrate concentrations were much greater (400- or 10000-fold) than the enzyme concentration, were at steady-state level. Thus all enzyme–substrate complexes would be formed at a constant rate at which they decomposed, e.g. $d[SE]/dt = 0$, $d[ES]/dt = 0$ and $d[SES]/dt = 0$. In this situation, the steady-state condition would be very close to the equilibrium condition if the rate of equilibration was very rapid compared with the rate at which the enzyme–substrate complex breaks down.

CYP3A4-mediated oxidation of DZ, TMZ and NDZ

To accurately evaluate the kinetic model and obtain kinetic parameters, approximately 40 different concentrations of DZ, TMZ or NDZ (ranging from 2 to 1200 μM) were used to generate an entire kinetic saturation curve by using cDNA-expressed CYP3A4. Eqn. (6), derived from the model in Scheme 3, was used to fit the experimental data. Similarly, in the metabolism of DZ and its derivatives, consumption of substrate was limited to less than 10 %, and the secondary metabolism of DZ was minimized. Sigmoidal plots of velocity versus substrate concentration for the formation of both metabolites were obtained by a non-linear least-squares regression (Figures 1A and 1B). The curve fit displayed the values in residual sums of squares and R^2, and kinetic estimates were determined by an iteration that was achieved at the best result (Table 1). Two sets of K_s values were achieved from sigmoidal velocity curves of TMZ and NDZ production in the metabolism of DZ by CYP3A4. In comparison, K_{s1}, K_{s2}, K_{s3} and K_{s4} (170, 421, 40 and 13 μM, respectively) measured from TMZ production were close to the corresponding values observed from NDZ production (125, 329, 28 and 9 μM, respectively), suggesting that these K_s values accurately describe the characteristics of substrate–enzyme binding affinities, although k values vary markedly for the formation of TMZ and NDZ. The results also indicated that K_{s1} and K_{s2} for two single-molecule-bound enzymes (SE and ES) were 4–36-fold larger than K_{s3} and K_{s4} for two-molecule-bound enzyme (SES), but rate constants k_α and k_β were 11–218-fold less than k_δ and k_γ. These values demonstrated that access and binding of the first molecule to either site in an active pocket of CYP3A4 could enhance co-operatively the binding affinity and reaction rate of a second molecule. In addition, introduction of a second molecule in an SES form alters initial features of binding and catalysis for the first molecule. Apparently, the change in kinetic characteristics is due to the co-operative binding of substrate molecules with the CYP3A4 enzyme. Thus the co-operative nature of enzyme that gives a sigmoidal response is described by the established four pairs of kinetic estimates.

TMZ and NDZ are products of 3-hydroxylation and N-demethylation of DZ, respectively, in which CYP3A4 plays a

Table 1 Kinetic estimates of sigmoidal saturation curves determined using eqn. (6)

Units of measurement are as follows: K_m (apparent), μM; V_{max}, nmol/min per nmol of P450; K_{S1-4}, μM; $k_{\alpha-\gamma}$, min^{-1}. K_m and V_{max} were determined by eqn. (2). Numbers in parentheses are standard errors. RSS, residual sum of squares; HLM, human liver microsomes.

Substrate	Product	Enzyme	K_m	V_{max}	K_{S1}	k_α	K_{S2}	k_β	K_{S3}	k_δ	K_{S4}	k_γ	RSS	R^2
DZ	TMZ	3A4			170 (135)	1.8 (1.4)	421 (233)	49.6 (10)	39.6 (24.7)	392 (94)	13.1 (5.3)	808 (182)	0.7611	0.999
	NDZ	3A4			125 (63)	5.6 (0.6)	329 (21)	4.5 (2.4)	28.1 (5.1)	111 (44)	8.9 (3.2)	49.2 (22.4)	1.020	0.997
TMZ	OX	3A4			482 (43)	10 (14)	830 (31)	29.6 (1.0)	23.3 (3.5)	76 (3.8)	16.5 (2.1)	76 (24)	0.3509	0.992
NDZ	OX	3A4			109 (29)	10.2 (4.1)	168 (31.5)	39.2 (9.3)	20.2 (31.5)	30.2 (22.2)	25.1 (2.3)	102 (33)	0.1327	0.992
DZ	TMZ	HLM			558 (112)	105 (41)	391 (98.7)	142.8 (53.8)	12.3 (5.7)	498 (242)	13.1 (4.5)	562 (135)	0.7333	0.996
	NDZ	HLM	94.6 (9.6)	1.27 (0.04)									0.1179	0.969
DZ	TMZ	HLM*	179.9 (8.8)	4.61 (0.9)									0.2514	0.999
	NDZ	HLM*	102 (8.0)	1.31 (0.03)									0.0711	0.988

* Anti-CYP3A4 mAb present.

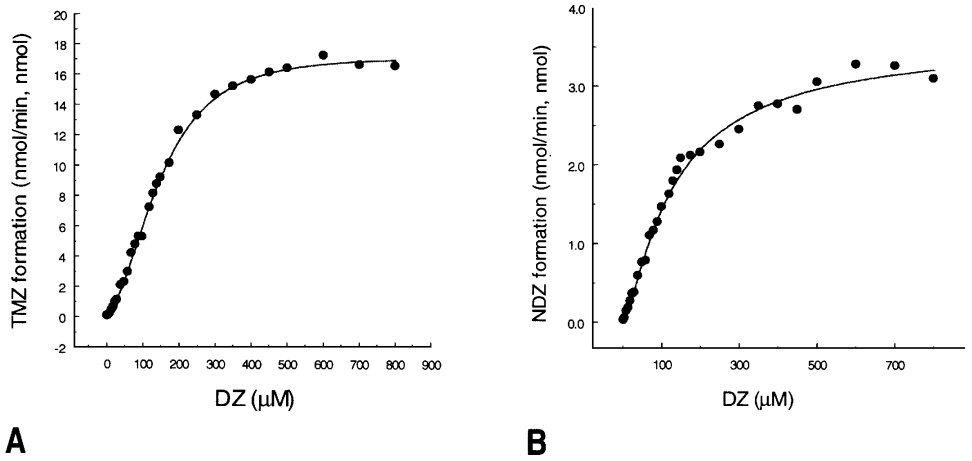

Figure 2 Sigmoidal (A) and hyperbolic (B) saturation curves of *v* versus [S] for TMZ and NDZ formation in the metabolism of DZ by human liver microsomes

Table 2 Kinetic estimates of sigmoidal saturation curves determined using eqn. (5)

Units of measurement are as follows: K_m (apparent), μM; and V_{max}, nmol/min per nmol of P450. Numbers in parentheses are standard errors. RSS, residual sum of squares; HLM, human liver microsomes.

Substrate	Product	Enzyme	K_{m1}	V_{max1}	K_{m2}	V_{max2}	RSS	R^2
DZ	TMZ	3A4*	356 (32)	2.1 (0.8)	11.4 (2.3)	24.2 (12.1)	1.2201	0.998
DZ	NDZ	3A4	284 (63)	1.4 (0.3)	18.7 (3.2)	4.8 (1.1)	0.3022	0.999
TMZ	OX	3A4	581 (139)	1.31 (0.12)	33.3 (1.4)	3.5 (1.5)	0.1145	0.998
NDZ	OX	3A4	164 (65)	3.7 (1.1)	24.4 (6.8)	4.8 (0.5)	0.3321	0.996
DZ	TMZ	HLM	491 (189)	8.9 (1.8)	19.4 (5.7)	16.7 (4.1)	2.0871	0.998

* cDNA-expressed CYP3A4.

role [17,19–21]. TMZ and NDZ can be further converted into OX that is eliminated from the body and/or undergoes glucuronidation (Scheme 2). Due to their structural similarities, studies on the metabolism of TMZ and NDZ by CYP3A4 was conducted to determine whether these substrates could serve as allosteric modifiers of the enzyme. Interestingly, the kinetic characteristics of CYP3A4 for both substrates appeared to be synonymous with those observed for DZ metabolism (Figures 1C and 1D). However, the k_γ and k_δ values, 76 min^{-1} for TMZ, and 30 and 102 min^{-1} for NDZ metabolism respectively, were lower than those (392 and 808 min^{-1}) for DZ metabolism (Table 1), suggesting that TMZ and NDZ were poorer substrates than DZ and that the binding co-operativity of the enzyme is substrate-dependent. Sigmoidal kinetics of TMZ and NDZ metabolism by CYP3A4 probably rely on the structures similar to DZ as a sigmoidal ligand, which accounts for the behaviour of the allosteric enzyme. In a similar fashion to DZ metabolism, the binding of a second molecule (TMZ or NDZ) to the enzyme to form an SES complex enhanced metabolism with decreased K_{S3} and K_{S4} and increased k_δ and k_γ values (Table 1).

Microsomal metabolism of DZ

Sigmoidal kinetics relating to the metabolism of DZ by human and rat liver microsomes have been reported in many studies [12,15–17]. Therefore, in the present study, the metabolism of DZ by pooled liver microsomes from six individuals was investigated with varying concentrations of substrate. Figures 2(A) and 2(B) show that human liver microsomes were capable of catalysing the metabolism of DZ to form TMZ and NDZ, and that the velocities for TMZ or NDZ formation were a function of substrate concentrations. Interestingly, our results indicated that, in a similar manner to recombinant CYP3A4, microsomes yielded a sigmoidal saturation profile for TMZ production but a hyperbolic profile for NDZ production. The kinetic parameters were determined by eqns. (6) and (2) (the Michaelis–Menten equation) respectively, as given in Table 1. Two different kinetic behaviours revealed in the metabolism of DZ by microsomes are suggestive of the major involvement of CYP3A4 for TMZ production and of other P450s for NDZ production.

In contrast with the present results, sigmoidal curves observed in the metabolism of DZ and its derivatives by CYP3A4 and human liver microsomes were tested to fit Korzekwa's model (eqn. 5). The kinetic estimates (e.g. K_{m1}, V_{max1}, K_{m2} and V_{max2}) were evaluated as seen in Table 2. The values of the K_{m1} for ES were found to be 7–25-fold greater than those of the K_{m2} for ESS ($K_{m1} > K_{m2}$). Accordingly, V_{max2} for ESS was 1.9–11-fold greater than V_{max1} ($V_{max2} > V_{max1}$). These results suggest that the single-substrate-bound enzyme complex (ES) displays a poorer binding affinity and catalytic capacity than the two-substrate-bound enzyme molecule (ESS), although the orientation between the two binding sites cannot be distinguished.

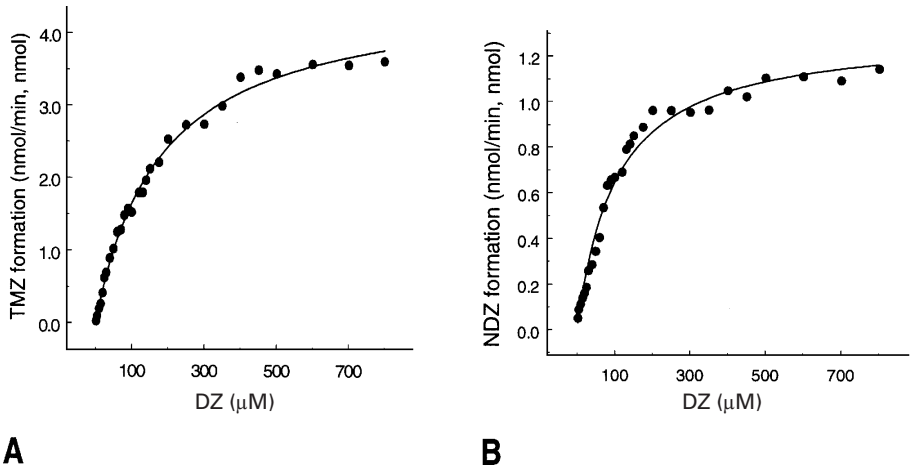

Figure 3 Hyperbolic saturation curve of *v* versus [S] for TMZ (A) and NDZ (B) formation in the metabolism of DZ by human liver microsomes in the presence of anti-CYP3A4 mAb

Anti-CYP3A4-mAb-mediated inhibition of the microsomal metabolism of DZ

To confirm that CYP3A4 plays a unique role in contributing to the co-operative reaction, an inhibitory mAb specific to CYP3A4 was utilized to assess the contribution of CYP3A4 to the sigmoidal kinetic characteristics of DZ metabolism in human liver microsomes. The optimal concentration of anti-CYP3A4 mAb (30 nM) was selected to achieve a maximal inhibition of CYP3A4-mediated oxidation of DZ ($> 90\%$). The kinetics of velocity versus substrate concentration in the microsomal metabolism of DZ were obtained in the presence of mAb (Figures 3A and 3B). The result showed that the velocities of TMZ and NDZ formation declined by comparison with those observed in the absence of anti-CYP3A4 mAb. Interestingly, when CYP3A4 activity was inhibited by the mAb, the nature of the kinetics of TMZ formation was no longer sigmoidal and changed to typical Michaelis–Menten kinetics (hyperbolic saturation curve). These results indicated that the sigmoidal curve for the microsomal production of TMZ in the absence of mAb is due mainly to CYP3A4 and the hyperbolic curve for NDZ production is due largely to other P450 isoforms (e.g. CYP2C8/9/19 and CYP2B6), rather than CYP3A4. Hence, K_m and V_{max} were determined to be 179.9 μM and 4.61 min^{-1} from a TMZ velocity curve and 102.0 μM and 1.31 min^{-1} from an NDZ velocity curve, respectively, by using the simple Michaelis–Menten equation (eqn. 2), as seen in Table 1. The slight difference in K_m and V_{max} values between TMZ and NDZ production kinetics apparently is an effect of multiple P450s contained in liver microsomes. This demonstrates that CYP3A4 in human liver containing multiple P450 isoforms is an allosteric enzyme responsible for the observed sigmoidal kinetics.

DISCUSSION

CYP3A4 appears to play a prominent role in the metabolism of drugs and xenobiotics in man. These substrates are generally large and highly lipophilic molecules and their K_m values vary markedly from 1 to 1500 μM. A number of workers have derived models for the active site of human P450s, based on either superposition of known substrates or sequence homologies with known crystal structures of P450s as templates. Others have explored P450 active sites using molecular probes [28]. In some cases, considerable changes in the active site region have been observed which reflect the differing substrate specificities, especially due to size and shape considerations. The CYP3A4 model shows a large active site with a well-defined access channel for substrates, in keeping with the known preferences of this enzyme for large, structurally diverse substrates. Even the cyclosporin molecule, which is of considerable size relative to other P450 substrates, is able to fit into the CYP3A4 site [29]. Due to the substrate diversity and kinetic multiplicity displayed by CYP3A4, it has been proposed that the CYP3A4 active site can accommodate two intermediate substrates at one time [9,14]. If both sites are co-operative, then the resulting kinetic characteristics of the SES species might differ from those observed for both single SE and ES species. Thus sigmoidal kinetics in many CYP3A4-catalysed reactions can be interpreted by the two-site model. This is a key hypothesis of the work described in the present report. Our experimental observations support the proposed two-site model that explains the substrate-activated sigmoidal kinetics of CYP3A4.

The *in vitro* kinetics of DZ metabolism by human liver microsomes have been investigated systematically and have revealed sigmoidal behaviour with respect to the nature of velocity versus substrate concentration [12,15–17]. The atypical kinetics are due clearly to the involvement of one or more allosteric enzymes among multiple P450s contained in liver. The substrate in this case also is a modifier or an activator of the enzyme. Our results indicate that CYP3A4 plays a unique role in the allosteric kinetics of DZ metabolism by human liver probed with an inhibitory mAb specific to CYP3A4. When DZ was metabolized by human liver microsomes, kinetics for TMZ formation (sigmoidal) appeared to be different from that for NDZ formation (hyperbolic; Figures 2A and 2B). The kinetic discrepancy of product specificity is attributed to the reaction preference of individual P450s, in which CYP3A4 is more favourable to the 3-hydroxylation, and CYP2B6 and CYP2C are favourable to the N-demethylation, of DZ. Substrate orientation favoured by different P450s may result in the product specificity. Because P450 exists in different expression environments, the kinetic estimates (e.g. K_s and k_p) determined for a specific P450 present in both the cDNA-expression system and human liver microsomes can be influenced by many factors. For example,

cytochrome b_5 may alter significantly or have no effect on the activity and affinity of the enzyme (k_p and K_S) [30–32]. Thus the changed kinetic estimates between the two preparations cannot be compared directly. However, the co-operative nature expressed by the specific P450 in both preparations could remain unaffected and their sigmoidal kinetic characteristics can be interpreted and evaluated using the model.

In this study, cDNA-expressed CYP3A4 displayed typical sigmoidal saturation curves in the metabolism of DZ, TMZ and NDZ. In general, K_{S1} and K_{S2} values for single-substrate-bound enzymes (SE and ES) were usually 10-fold greater than K_{S3} and K_{S4} for the two-substrate-bound enzyme (SES; Table 1). This suggests that the binding of the first molecule expressed by K_{S1} or K_{S2} increases the binding affinity of the vacant site (K_{S3} or K_{S4}) for a second molecule. Due to the co-operative binding of substrate and the shift in K_S value, the changes of the k value also can take place. Our results showed that k_δ and k_γ were always greater than k_α and k_β respectively for all sigmoidal reactions, indicating that co-operativity can increase markedly the catalytic activity of the CYP3A4 enzyme, e.g. k_δ (392 min^{-1}) and k_γ (808 min^{-1}) were 217- and 16-fold higher in TMZ formation of DZ metabolism than k_α (1.8 min^{-1}) and k_β (49.6 min^{-1}) respectively. These are due probably to a conformational change in the enzyme, which binds tightly to two substrates in a SES form and allows the substrate to be metabolized readily. The model also describes the kinetic discrepancy between two single-bound sites on the enzyme. For example, in the conversion of DZ into TMZ by CYP3A4 (Table 1), K_{S2} and k_β for ES were 2.5- and 28-fold greater than K_{S1} and k_α for SE, respectively, implying that ES will more readily dissociate to E and S, and form product (P). Similarly, the K_{S3} and k_δ were 3-fold greater and 2-fold less than K_{S4} and k_γ, respectively, indicating that the binding of S to ES is more tight than that of S to SE and that the rate of SES $\rightarrow$ ES + P is faster than that of SES $\rightarrow$ SE + P.

Koley et al. [33,34] have suggested that CYP3A4 exists as multiple, kinetically distinct and interconvertible conformers in the microsomal membrane. The conformers have been shown to differ in their substrate-binding specificities using CO-binding kinetics. The kinetics of CYP3A4 expressed in both human liver microsomes and baculovirus-infected Sf9 insect cells can be modulated by specific substrates via changes in CYP3A4 conformation/dynamics that either accelerate (nifedipine and erythromycin) or reduce (quinidine, testosterone and warfarin) the binding rate, and/or via steric effects that reduce the rate [33,34]. These observations provide a basis for the recognition by CYP3A4 with a wide range of structurally diverse substrates. However, it would be complicated to interpret enzyme co-operativity by a kinetic solution for multiple conformers of a P450 enzyme, due to the multiplicity of conformers, number of allosteric sites and successive interconversion between the conformers. In addition, co-operative characteristics of each individual conformer, membrane condition, CYP-OR and substrate used may change the ratio between conformers. Importantly, allosteric kinetics exhibited by CYP3A4 for the substrates have not been characterized.

Ueng et al. reported recently that the metabolism of testosterone, 17β-oestradiol, amitriptyline and aflatoxin B1 with CYP3A4 in a reconstituted system was confirmed to exhibit allosteric kinetics [5]. The Hill model was used to consider an enzyme with two identical and distinct substrate-binding sites, one catalytic site and one effector site, respectively. The effector site may change the binding affinity and catalytic ability of active site. Thus sigmoidal kinetics were fitted and determined by the Hill equation (eqn. 4). However, there are several limitations when applying the Hill equation to the P450-catalysed reactions that display sigmoidal kinetics. First, the Hill equation is more appropriate to explain an allosteric enzyme that contains more than two binding sites. Sigmoidal kinetics for a two-site model can be determined easily and accurately by eqn. (3). The α value in eqn. (3) is a determinant of the sigmoidicity of the velocity curve and K_S is an estimate of K_m. Second, the Hill equation requires high co-operativity of substrate binding. Otherwise the velocity equation derived from multiple binding sites will not reduce to the Hill equation and n in the Hill equation will no longer equal the actual number of substrate-binding sites. For example, if the co-operativity of substrate binding to an enzyme with two sites is dependent upon the SES species to generate a major portion of the velocity curve between 10 and 90 % of V_{max}, then the velocity data can be made to fit the Hill equation. Third, as mentioned above, the constant K' represents neither K_m nor C_{50} (or S_{50}), except for when $n = 1$. Fourth, the Hill equation (eqn. 3) in a two-site model assumes that binding affinities for two sites (K_S for SE and ES) are identical, as shown in Scheme 1. This may not be the case for P450 enzymes, monomers of asymmetric structure with one active site. Our model in Scheme 3 suggests that if two binding sites are distinct and co-operative, the binding relationship between enzyme and substrate can be expressed accurately by K_{S1} for SE, K_{S2} for ES, and K_{S3} and K_{S4} for SES species respectively, and rate constants (k) may vary with the change in the corresponding K_S values. Therefore, the fit of the Hill equation for sigmoidal kinetics is one of many allosteric expressions.

Most recently, the allosteric mechanism of CYP3A4 was explained in part by the study of site-directed mutagenesis [7]. The results have shown that the sigmoidal curve of steroid hydroxylation by CYP3A4 is shifted to hyperbolic kinetics when replacing residues Leu-211 and Asp-214 with the larger Phe and Glu (L211F and D214E) respectively, suggesting that the residues could be a portion of the effector-binding site that is required for co-operativity. One steroid (testosterone) as an effector for wild-type CYP3A4 stimulated the hydroxylation of another as a substrate (progesterone), whereas it inhibited the hydroxylation activity of the L211F/D214E mutant (competitive inhibition). It is believed that residues 211 and 214 may play a role in defining a second site for binding of steroid as an effector and thereby indicate that binding of effector in an active site could alter the metabolic profiles of a substrate, e.g. K_m and V_{max}.

Interestingly, the kinetic equations for the two-site model that were derived recently by Korzekwa et al. explain several non-hyperbolic saturation curves in P450-catalysed reactions [9]. In this study, sigmoidal kinetic curves were observed for the oxidations of carbamazepine, naphthalene and dapsone by different P450s. Using the two-site model, kinetic constants were determined and expressed for different substrate–enzyme species, e.g. K_{m1} and V_{max1} for ES and K_{m2} and V_{max2} for ESS. The parameters presented by allosteric enzymes exhibited values of $V_{max2} > V_{max1}$ and $K_{m1} < \text{or} > K_{m2}$, depending on different estimations of initial parameters, suggesting that allosteric binding changes the kinetic characteristics of the enzyme for a specific substrate. In order to compare our results, Korzekwa et al.'s model was assessed to generate kinetic estimates and was shown to have a good curve fit (Table 2). The kinetic estimation was in general agreement with our observations, showing that the ES complex has both poorer binding affinity and catalytic capacity than the ESS ($K_{m1} > K_{m2}$ and $V_{max1} < V_{max2}$). The increase in binding affinity and catalytic rate of the CYP3A4 for the second substrate molecule is probably attributed to binding of the first substrate to the active site, which induces an enzyme co-operativity. Since the model defines the binding of S to E with no orientation difference (SE = ES) and the assumptions for the

two models are different, the features of kinetic estimates are not equivalent.

In a steady-state treatment, K_m values are considered in Scheme 3 to express $K_{m1} = (k_{-1}+k_\alpha)/k_1$, $K_{m2} = (k_{-2}+k_\beta)/k_2$, $K_{m3} = (k_{-3}+k_\delta)/k_3$ and $K_{m4} = (k_{-4}+k_\gamma)/k_4$. If rate constants are very small relative to their corresponding dissociation constants, k_α, k_β, k_δ and k_γ can be negligible and, therefore, dissociation constants (K_s) in eqn. (6) are close to their respective Michaelis constants (K_m), e.g. $K_{m1} \approx K_{s1} = k_{-1}/k_1$, $K_{m2} \approx K_{s2} = k_{-2}/k_2$, $K_{m3} \approx K_{s3} = k_{-3}/k_3$ and $K_{m4} \approx K_{s4} = k_{-4}/k_4$, reflecting the magnitude of substrate binding. Accordingly, four corresponding rate constants (k) can be produced. The four pairs of K_s and k constants can be defined to characterize the nature of the allosteric enzyme, leading to a better understanding of co-operative binding of two substrate molecules in the inner portions of an active site. The experimental results have provided a support for our hypothesis.

Furthermore, since the enzyme reaction is closed and forms a cycle, as shown in Scheme 3, the relationship between kinetic constants can be expressed as $K_{s1}K_{s3} = K_{s2}K_{s4}$. Thus the kinetic parameters derived from the model can be compared to ascertain if the relationship between K_s values exists and supports our model. Table 1 shows that the values ($K_{s1}K_{s3}$) for CYP3A4-mediated oxidations of DZ, TMZ and NDZ are generally comparable with those of $K_{s2}K_{s4}$, although deviations of approximately 16–32 % were observed.

In summary, CYP3A4 exhibited sigmoidal kinetic characteristics in the oxidation of DZ, TMZ and NDZ. The model for two-substrate binding to an active site was developed to derive a velocity equation under a rapid equilibrium treatment. The estimates of kinetic parameters provide more insights into two co-operative substrate-binding sites within a CYP3A4 active site.

We gratefully acknowledge Dr. Kenneth R. Korzekwa for valuable discussion.

REFERENCES

1 Gonzalez, F. J. (1989) Pharmacol. Rev. **40**, 243–288
2 Guengerich, F. P. (1990) Crit. Rev. Biochem. Mol. Biol. **25**, 97–153
3 Guengerich, F. J., Gillam, E. M. J., Martin, M. V., Baba, T., Kim, B. R., Raney, K. D. and Yun, C. H. (1988) in Assessment of the Use of Single Cytochrome P450 Enzymes in Drug Research (Waterman, M. R. and Hildebrand, M., eds.), pp. 161–186, Springer, Berlin
4 Gonzalez, F. J. and Gelboin, H. V. (1994) Drug Metab. Rev. **26**, 165–183
5 Ueng, Y. F., Kuwabara, T., Chun, Y. J. and Guengerich, F. P. (1997) Biochemistry **36**, 370–381
6 Schwab, G. E., Raucy, J. L. and Johnson, E. F. (1998) Mol. Pharmacol. **33**, 493–499
7 Harlow, G. R. and Halpert, J. R. (1998) Proc. Natl. Acad. Sci. U.S.A. **95**, 6636–6641
8 Kerr, B. M., Thummel, K. E., Wurden, C. J., Klein, S. M., Kroetz, D. L., Gonzalez, F. J. and Levy, R. H. (1994) Biochem. Pharmacol. **47**, 1969–1979
9 Korzekwa, K. R., Krishnamachary, N., Shou, M., Ogai, A., Parise, R. A., Rettie, A. E., Gonzalez, F. J. and Tracy, T. S. (1998) Biochemistry **37**, 4137–4147
10 Schmider, J., Greenblatt, D. J., von-Moltke, L. L., Harmatz, J. S. and Shader, R. I. (1955) J. Pharmacol. Exp. Ther. **275**, 592–597
11 Atkinson, D. E., Hathaway, J. A. and Smith, E. C. (1965) J. Biol. Chem. **240**, 2682–2693
12 Andersson, T., Miners, J. O., Veronese, M. E. and Birkett, D. J. (1994) Br. J. Clin. Pharmacol. **38**, 131–137
13 Zomorodi, K., Carlile, D. J. and Houston, J. B. (1995) Xenobiotica **25**, 907–916
14 Shou, M., Grogan, J., Mancewicz, J. A., Krausz, K. W., Gonzalez, F. J., Gelboin, H. V. and Korzekwa, K. R. (1994) Biochemistry **33**, 6450–6455
15 Bertilsson, L., Baillie, T. A. and Reviriego, J. (1990) Pharmacol. Ther. **45**, 85–91
16 Hooper, W. D., Watt, J. A., McKinnon, G. E. and Reilly, P. E. (1992) Eur. J. Drug Metab. Pharmacokinet. **17**, 51–59
17 Yang, T. J., Shou, M., Korzekwa, K. R., Gonzalez, F. J., Gelboin, H. V. and Yang, S. K. (1998) Biochem. Pharmacol. **55**, 889–896
18 Jung, F., Richardson, T. H., Raucy, J. L. and Johnson, E. F. (1997) Drug Metab. Dispos. **25**, 133–139
19 Neville, C. F., Ninomiya, S., Shimada, N., Kamataki, T., Imaoka, S. and Funae, Y. (1993) Biochem. Pharmacol. **45**, 59–65
20 Ono, S., Hatanaka, T., Miyazawa, S., Tsutsui, M., Aoyama, T., Gonzalez, F. J. and Satoh, T. (1996) Xenobiotica **26**, 1155–1166
21 Reilly, P. E., Thompson, D. A., Mason, S. R. and Hooper, W. D. (1990) Mol. Pharmacol. **37**, 767–774
22 Gelboin, H. V., Krausz, K. W., Goldfarb, I., Buters, J. T. M., Yang, S. K., Gonzalez, F. J., Korzekwa, K. R. and Shou, M. (1995) Biochem. Pharmacol. **55**, 1841–1850
23 Gonzalez, F. J., Schmid, B. J., Umeno, M., McBride, O. W., Hardwick, J. P., Meyer, U. A., Gelboin, H. V. and Idle, J. R. (1988) DNA **7**, 79–86
24 Yamano, S., Aoyama, T., McBride, O. W., Hardwick, J. P., Gelboin, H. V. and Gonzalez, F. J. (1989) Mol. Pharmacol. **36**, 83–88
25 Omura, T. and Sato, R. (1964) J. Biol. Chem. **239**, 2370–2379
26 Wang, P. P., Beaune, P., Kaminsky, L. S., Dannan, G. A., Kadlubar, F. F., Larrey, D. and Guengerich, F. P. (1983) Biochemistry **22**, 5375–5383
27 Marquardt, D. W. (1963) J. Soc. Indust. Appl. Math. **11**, 431–441
28 Swanson, B. A., Dutton, D. R., Lunetta, J. M., Yang, C. S. and Ortiz de Montellano, P. R. (1991) J. Biol. Chem. **266**, 19258–19310
29 Lewis, D. F. V. (1996) in Cytochromes P450: Metabolic and Toxicological Aspects (Ioannides, C., ed.), pp. 355–398, CRC Press, Boca Raton
30 Usanov, S. A., Honkakoski, P., Lang, M. and Hanninen, O. (1990) Biokhimiia **55**, 995–1007
31 Jansson, I., Tamburini, P. P., Favreau, L. V. and Schekma, J. B. (1985) Drug Metab. Dispos. **13**, 453–458
32 Patten, C. J., Ishizaki, H., Aoyama, T., Lee, M., Ning, S. M., Huang, W., Gonzalez, F. J. and Yang, C. S. (1992) Arch. Biochem. Biophys. **299**, 163–171
33 Koley, A. P., Buters, J. T. M., Robinson, R. C., Markowitz, A. and Friedman, F. K. (1995) J. Biol. Chem. **270**, 5014–5018
34 Koley, A. P., Robinson, R. C. and Friedman, F. K. (1996) Biochimie **78**, 706–713

Received 16 December 1998/16 March 1999; accepted 31 March 1999